Available online at www.sciencedirect.com

SCIENCE DIRECT®

Journal of Sound and Vibration 282 (2005) 249–264

JOURNAL OF SOUND AND VIBRATION

www.elsevier.com/locate/jsvi

Dynamic analysis of planar closed-frame structures

Hai-Ping Lin*, Jian-Da Wu

Department of Mechanical & Automation Engineering, Da-Yeh University, 112 Shan-Jiau Road, Da-Tsuen, Chang-hua, Taiwan 51505, ROC

Received 8 September 2003; accepted 18 February 2004
Available online 17 September 2004

Abstract

An eigenanalysis problem concerning planar closed-frame structures is investigated. A hybrid analytical/numerical method is proposed that permits an efficient dynamic analysis of these structures. The method utilizes a numerical implementation of a transfer matrix solution to the analytical equation of motion. By using the Timoshenko beam theory, by analyzing the transverse and longitudinal motions of each segment simultaneously, and by considering the compatibility requirements across each frame angle, the undetermined variables of the entire frame structure system can be reduced to six. Then, by considering the relationship between the first segment and the last segment in the closed structure, the eigenvalues can be obtained by the existence of the non-trivial solutions. The main feature of this method is decreasing the dimensions of the matrix involved in the finite element methods and various other analytical methods.

1. Introduction

Frame structures are usually used in the engineering designs, i.e., cranes, bridges, aerospace structures, etc. The dynamic behaviors of frame structures can be predicted by using various analytical and numerical methods such as the dynamic stiffness method (DSM) and the finite element method (FEM). The DSM employs the solutions of the governing equations under harmonic nodal excitations as shape functions to formulate the analytical stiffness matrix. The method requires the closed-form solutions of the governing equations and which restricts the

*Corresponding author. Tel.: +886-4-8511888 ext. 2586; fax: +886-4-8511895.
E-mail address: linhp@mail.dyu.edu.tw (H.-P. Lin).

0022-460X/$ - see front matter © 2004 Published by Elsevier Ltd.
doi:10.1016/j.jsv.2004.02.027

application areas [1]. The FEM has been used very commonly in recent years in this field. However, the FEM requires a large amount of computer memory and computation time, since it requires many degrees of freedom for solving dynamic problems accurately for these structures [2,3]. To solve this problem, various methods have been studied to overcome these disadvantages [2,4,5]. In most of the previous studies, the model of the Euler–Bernoulli beam theory by deriving the differential equation and the associated boundary conditions for a basic uniform Euler–Bernoulli beam are often used and discussed. The model of an Euler–Bernoulli beam is simpler; however, it has some restrictions in its applications, especially, in cases of short beams [6]. Some research has also studied the different results between the models of the Euler–Bernoulli beam theory and the Timoshenko beam theory. Finally, it is possible to evaluate natural frequencies simply by finding roots of the *high-order determinant* of the coefficient matrix of the linear system if the accuracy of the eigensolutions is required.

This investigation presents a hybrid analytical/numerical method that permits an efficient computation of the eigensolutions for closed-frame structures by using the Timoshenko beam model. The method is based on partitioning a closed-frame structure to the sub-beam segments. By considering the transverse and longitudinal motions of each segment simultaneously, and by the compatibility requirements across each frame angle, the relationships among the six integration constants of the eigenfunctions between adjacent sub-beams can be determined. By using the transfer matrix methods [11–13], as a consequence, the entire system has only six unknown constants. Then, by considering the relationship between the first segment and the last segment in this closed structure, the eigenvalues can be obtained by the existence of the non-trivial solutions.

2. Theoretical model

A typical planar closed-frame structure with K frame angles $\theta_1, \theta_2, \ldots, \theta_k$ is shown in Fig. 1. This structure is partitioned into K components at the angle positions, thereby enabling a

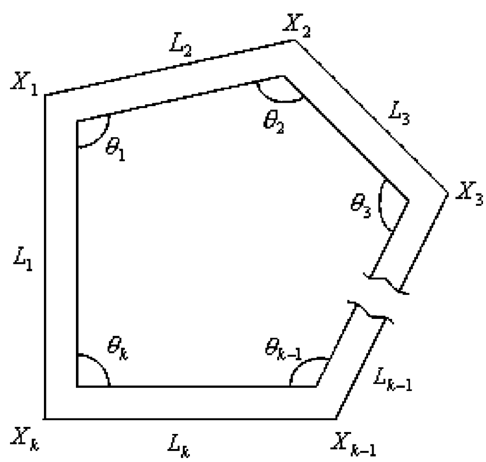

Fig. 1. A planar closed-frame structure with K frame angles $\theta_1, \theta_2, \ldots, \theta_K$ located at positions $X_1, X_2 \ldots, X_k$, respectively, with sub-beams $L_1, L_2, \ldots, L_K$ where $L_1 + L_2 + \cdots + L_K = L$.

sub-structure approach. There are K sub-beams with lengths $L_1, L_2, \ldots, L_k$ and the positions of the frame angles are located by $X_1, X_2, ..., X_K$, respectively, in Fig. 1. When doing a vibration analysis of the system presented in this article, each component member (sub-beam) is analyzed by its transverse and longitudinal motions, respectively. Let the X-axis represent the longitudinal direction and the Y-axis represent the transverse direction of each component member; then, the transverse vibration by Timoshenko beam theory and the axial vibration of a rod is considered. The vibration amplitudes of the transverse and longitudinal displacements of component i (sub-beam) are denoted by $Y_{(i)}(X,T)$ and $U_{(i)}(X,T)$ on the interval $X_{i-1}<X<X_i$, where the sub-index i represents the ith segment and $i=1,2,...,K$, as shown in Fig. 2. The entire system is now divided into K segments and the total length of this planar closed-frame system is $L(=L_1+L_2+...+L_K)$. From Ref. [6–10], the equations of motion for each segment, assumed with a uniform cross-section, are

Transverse motion:

$$EI\frac{\partial^4 Y_{(i)}(X,T)}{\partial X^4}+\rho A\frac{\partial^2 Y_{(i)}(X,T)}{\partial T^2}-\rho I\left(1+\frac{E}{kG}\right)\frac{\partial^4 Y_{(i)}(X,T)}{\partial T^2\partial X^2}+\frac{\rho^2 I}{kG}\frac{\partial^4 Y_{(i)}(X,T)}{\partial T^4}=0,$$
$$X_{i-1}<X<X_i,\quad i=1,2,...,K. \tag{1}$$

Slope due to bending:

$$EI\frac{\partial^4 \Phi_{(i)}(X,T)}{\partial X^4}+\rho A\frac{\partial^2 \Phi_{(i)}(X,T)}{\partial T^2}-\rho I\left(1+\frac{E}{kG}\right)\frac{\partial^4 \Phi_{(i)}(X,T)}{\partial T^2\partial X^2}+\frac{\rho^2 I}{kG}\frac{\partial^4 \Phi_{(i)}(X,T)}{\partial T^4}=0,$$
$$X_{i-1}<X<X_i,\quad i=1,2,...,K. \tag{2}$$

Longitudinal motion:

$$E\frac{\partial^2 U_{(i)}(X,T)}{\partial X^2}-\rho\frac{\partial^2 U_{(i)}(X,T)}{\partial T^2}=0,\qquad X_{i-1}<X<X_i,\quad i=1,2,...,K, \tag{3}$$

where $\Phi_{(i)}(X,T)$ is the rotation of the line elements along the centerline only due to bending, E is Young's modulus of the material, I is the moment of inertia of the beam cross-section, ρ is the density of material, A is the cross-section area of the beam, G is the shear modulus, k is the Timoshenko shear coefficient, which may also be a function of Poisson's ratio v [6], and T is the time. The shear force V and bending moment M at each cross-section of the beam can be

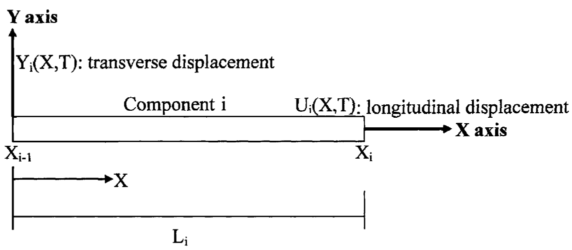

Fig. 2. Transverse and longitudinal motions of a segment.

expressed as [6]

$$V(X,T) = -kGA[Y'(X,T) - \Phi(X,T)]$$

$$M(X,T) = EI\Phi'(X,T).$$

The transverse and the longitudinal motions at the end of the segment before each frame angle constrain the motions of the adjacent segment after the same frame angle. Therefore, the "compatibility conditions" enforcing continuities of the displacement fields (both in transverse and longitudinal), the slope, the bending moment, the shear force and axial force, respectively, across each frame angle θ_i, as shown in Fig. 3a (displacements) and 3b (forces), and can be

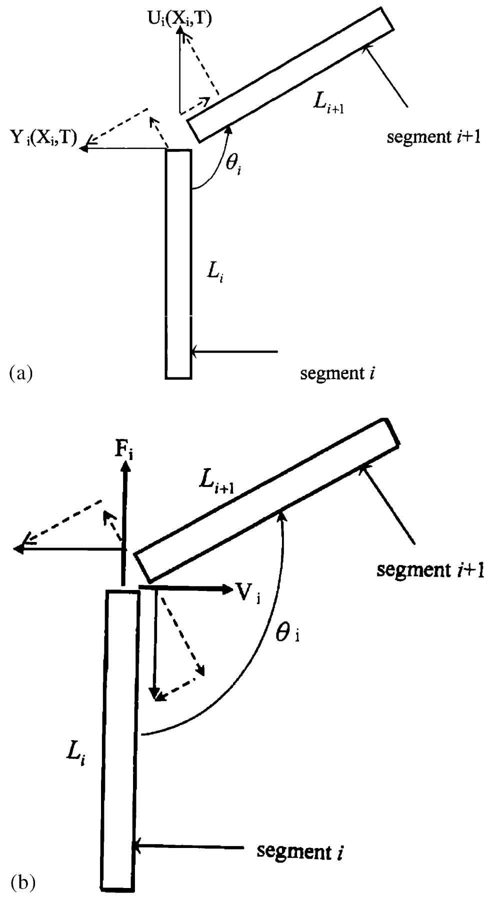

Fig. 3. (a) Displacement compatibility requirements across ith frame angle θ_i: Y_i and U_i are transverse and longitudinal displacements of segment i at position X_i. (b) Force compatibility requirements across ith frame angle θ_i: V_i and F_i are shear and axial forces of segment i at position X_i.

expressed as [13]

$$Y_{(i+1)}(X_i^+, T) = -Y_{(i)}(X_i^-, T)\cos\theta_i + U_{(i)}(X_i^-, T)\sin\theta_i, \quad \text{displacement continuity,} \tag{4a}$$

$$U_{(i+1)}(X_i^+, T) = -Y_{(i)}(X_i^-, T)\sin\theta_i - U_{(i)}(X_i^-, T)\cos\theta_i, \quad \text{displacement continuity,} \tag{4b}$$

$$Y'_{(i+1)}(X_i^+, T) = Y'_{(i)}(X_i^-, T), \quad \text{slope continuity} \tag{4c}$$

$$EI\,\Phi'_{(i+1)}(X_i^+, T) = EI\,\Phi'_{(i)}(X_i^-, T), \quad \text{moment continuity} \tag{4d}$$

$$\begin{aligned} -kGA\,[Y'_{(i+1)}(X_i^+, T) - \Phi_{(i+1)}(X_i^+, T)] &= kGA\,[Y'_{(i)}(X_i^-, T) - \Phi_{(i)}(X_i^-, T)]\cos\theta_i \\ &\quad - EAU'_{(i)}(X_i^-, T)\sin\theta_i, \quad \text{shear continuity,} \end{aligned} \tag{4e}$$

$$\begin{aligned} EAU'_{(i+1)}(X_i^+, T) = &- kGA\,[Y'_{(i)}(X_i^-, T) - \Phi_{(i)}(X_i^-, T)]\sin\theta_i \\ &- EAU'_{(i)}(X_i^-, T)\cos\theta_i, \quad \text{axial force continuity,} \end{aligned} \tag{4f}$$

where the symbols X_i^+ and X_i^- denote the locations just above and below the angle position X_i. All the assumptions in the above compatibility conditions are the same as the traditional analysis of the transverse vibrations of a Timoshenko beam and the axial vibrations of a rod. The frame angles are also assumed to be unchanged during the motions of the frame.

In the above, the following quantities are introduced:

$$y_{(i)} = \frac{Y_{(i)}}{L}, \;\; \phi_{(i)} = \Phi_{(i)}, \;\; x = \frac{X}{L}, \;\; u_{(i)} = \frac{U_{(i)}}{L}, \;\; t = \frac{T}{\sqrt{L}}, \;\; l_i = \frac{L_i}{L}, \;\; x_i = \frac{X_i}{L}. \tag{5a−5g}$$

Thus, in each segment, Eqs. (1)–(3) can then be expressed in non-dimensional form as

$$\frac{EI}{L^3}\frac{\partial^4 y_{(i)}(x,t)}{\partial x^4} + \rho A\frac{\partial^2 y_{(i)}(x,t)}{\partial t^2} - \frac{\rho I}{L^2}\left(1 + \frac{E}{kG}\right)\frac{\partial^4 y_{(i)}(x,t)}{\partial t^2 \partial x^2} + \frac{\rho^2 I}{kGL}\frac{\partial^4 y_{(i)}(x,t)}{\partial t^4} = 0, \quad x_{i-1} < x < x_i, \quad i = 1, 2, ..., K. \tag{6}$$

$$\frac{EI}{L^3}\frac{\partial^4 \phi_{(i)}(x,t)}{\partial x^4} + \rho A\frac{\partial^2 \phi_{(i)}(x,t)}{\partial t^2} - \frac{\rho I}{L^2}\left(1 + \frac{E}{kG}\right)\frac{\partial^4 \phi_{(i)}(x,t)}{\partial t^2 \partial x^2} + \frac{\rho^2 I}{kGL}\frac{\partial^4 \phi_{(i)}(x,t)}{\partial t^4} = 0, \quad x_{i-1} < x < x_i, \quad i = 1, 2, ..., K. \tag{7}$$

$$\frac{E}{L}\frac{\partial^2 u_{(i)}(x,t)}{\partial x^2} - \rho\frac{\partial^2 u_{(i)}(x,t)}{\partial t^2} = 0, \quad x_{i-1} < x < x_i, \quad i = 1, 2, ..., K. \tag{8}$$

The non-dimensional "compatibility conditions" across each frame angle are (from Eqs. (4a) to (4f))

$$y_{(i+1)}(x_i^+,t) = -y_{(i)}(x_i^-,t)\cos\theta_i + u_{(i)}(x_i^-,t)\sin\theta_i, \tag{9a}$$

$$u_{(i+1)}(x_i^+,t) = -y_{(i)}(x_i^-,t)\sin\theta_i - u_{(i)}(x_i^-,t)\cos\theta_i, \tag{9b}$$

$$y'_{(i+1)}(x_i^+,t) = y'_{(i)}(x_i^-,t), \tag{9c}$$

$$\phi'_{(i+1)}(x_i^+,t) = \phi'_{(i)}(x_i^-,t), \tag{9d}$$

$$y'_{(i+1)}(x_i^+,t) - \phi_{(i+1)}(x_i^+,t) = -[y'_{(i)}(x_i^-,t) - \phi_{(i)}(x_i^-,t)]\cos\theta_i + \frac{E}{kG}u'_{(i)}(x_i^-,t)\sin\theta_i, \tag{9e}$$

$$u'_{(i+1)}(x_i^+,t) = -\frac{kG}{E}[y'_{(i)}(x_i^-,t) - \phi_{(i)}(x_i^-,t)]\sin\theta_i - u'_{(i)}(x_i^-,t)\cos\theta_i,$$
$$\text{where } i = 1,2,\ldots,K. \tag{9f}$$

3. Calculation of eigensolutions

Using the separable solutions $y_{(i)}(x,t) = w_{(i)}(x)\,\mathrm{e}^{\mathrm{j}\omega t}$ and $u_{(i)}(x,t) = v_{(i)}(x)\mathrm{e}^{\mathrm{j}\omega t}$ in Eqs. (6) and (8) leads to an associated eigenvalue problem

$$w''''_{(i)}(x) + (\sigma+\tau)w''_{(i)}(x) - (\alpha - \sigma\tau)w_{(i)}(x) = 0, \quad x_{i-1} < x < x_i, \quad i = 1,2,\ldots,K, \tag{10}$$

$$v''_{(i)}(x) + \gamma^2 v_{(i)}(x) = 0, \quad x_{i-1} < x < x_i, \quad i = 1,2,\ldots,K, \tag{11}$$

where

$$\sigma = \frac{\rho L\omega^2}{E}, \ \tau = \frac{\rho L\omega^2}{kG}, \ \alpha = \frac{A\rho L^3\omega^2}{EI} \quad \text{and} \quad \gamma^2 = \frac{\rho L\omega^2}{E}\sigma. \tag{12a-12d}$$

The general solutions of Eqs. (10) and (11), for each segment, are [10]

$$w_{(i)}(x) = A_i\cosh\lambda_1(x-x_{i-1}) + B_i\sinh\lambda_1(x-x_{i-1}) + C_i\cos\lambda_2(x-x_{i-1}) + D_i\sin\lambda_2(x-x_{i-1}),$$

$$x_{i-1} < x < x_i, \quad i = 1,2,\ldots,K, \tag{13}$$

$$v_{(i)}(x) = E_i\sin\gamma(x-x_{i-1}) + F_i\cos\gamma(x-x_{i-1}), \quad x_{i-1} < x < x_i, \quad i = 1,2,\ldots,K, \tag{14}$$

where

$$\lambda_1 = \left(\sqrt{\left(\frac{\sigma-\tau}{2}\right)^2 + \alpha} - \frac{\sigma+\tau}{2}\right)^{1/2}, \quad \lambda_2 = \left(\sqrt{\left(\frac{\sigma-\tau}{2}\right)^2 + \alpha} + \frac{\sigma+\tau}{2}\right)^{1/2}. \tag{15a, b}$$

Similarly, from Eq. (7), by letting $\phi_{(i)}(x,t) = \varphi_{(i)}(x)e^{j\omega t}$, a general solution for $\varphi_{(i)}(x)$ is derived as [10]

$$\begin{aligned}\varphi_{(i)}(x) = {} & B_i q_1 \cosh\ \lambda_1(x - x_{i-1}) + A_i q_1 \sinh\ \lambda_1(x - x_{i-1}) \\ & - D_i q_2 \cos\ \lambda_2(x - x_{i-1}) + C_i q_2 + \sin\ \lambda_2(x - x_{i-1}),\end{aligned}$$

$$x_{i-1} < x < x_i, \quad i = 1, 2, \ldots, K, \tag{16}$$

where

$$q_1 = (\lambda_3^2 + \lambda_1^2)/\lambda_1, \qquad q_2 = (\lambda_3^2 - \lambda_2^2)/\lambda_2, \qquad \lambda_3 = (\rho L\omega^2/kG)^{1/2}. \tag{17a−c}$$

In the above equations (Eqs. (13), (14) and (16)), A_i, B_i, C_i, D_i, E_i and F_i are constants associated with the ith segment ($i = 1, 2, \ldots, K$).

From Eqs. (9a) to (9f), the corresponding compatibility conditions across each frame angle lead to

$$w_{(i+1)}(x_i^+) = -w_{(i)}(x_i^-)\cos\theta_i + v_{(i)}(x_i^-)\sin\theta_i, \tag{18a}$$

$$v_{(i+1)}(x_i^+) = -w_{(i)}(x_i^-)\sin\theta_i - v_{(i)}(x_i^-)\cos\theta_i, \tag{18b}$$

$$w'_{(i+1)}(x_i^+) = w'_{(i)}(x_i^-), \tag{18c}$$

$$\varphi'_{(i+1)}(x_i^+) = \varphi'_{(i)}(x_i^-), \tag{18d}$$

$$w'_{(i+1)}(x_i^+) - \varphi_{(i+1)}(x_i^+) = -[w'_{(i)}(x_i^-) - \varphi_{(i)}(x_i^-)]\cos\theta_i + \frac{E}{kG}v'_{(i)}(x_i^-)\sin\theta_i, \tag{18e}$$

$$\begin{aligned}v'_{(i+1)}(x_i^+) = {} & -\frac{kG}{E}[w'_{(i)}(x_i^-) - \varphi_{(i)}(x_i^-)]\sin\theta_i - v'_{(i)}(x_i^-)\cos\theta_i, \\ & \text{for}\ \ i = 1, 2, \ldots, K.\end{aligned} \tag{18f}$$

A closed-form solution to this eigenvalue problem can be obtained by employing the transfer matrix method [11–13]. The constants in the $(i+1)$th segment of Eqs. (13), (14) and (16), A_{i+1}, B_{i+1}, C_{i+1}, D_{i+1}, E_{i+1}, F_{i+1}, are related to those in the ith segment (A_i, B_i, C_i, D_i, E_i and F_i) through the compatibility conditions in Eqs. (18a)–(18f); thus, these constants can be expressed as

$$\begin{Bmatrix} A_{i+1} \\ B_{i+1} \\ C_{i+1} \\ D_{i+1} \\ E_{i+1} \\ F_{i+1} \end{Bmatrix} = \begin{bmatrix} t_{11} & t_{12} & t_{13} & t_{14} & t_{15} & t_{16} \\ \vdots & & & & & \\ \vdots & & & & & \\ \ldots\ldots & & & & ..t_{66} & t_{66} \end{bmatrix}^{(i)} \begin{Bmatrix} A_i \\ B_i \\ C_i \\ D_i \\ E_i \\ F_i \end{Bmatrix} = \mathbf{T}_{6\times 6}^{(i)} \begin{Bmatrix} A_i \\ B_i \\ C_i \\ D_i \\ E_i \\ F_i \end{Bmatrix}, \qquad i = 1, 2, \ldots, K-1, \tag{19}$$

where $\mathbf{T}^{(i)}_{6\times 6}$ is the 6×6 transfer matrix which depends on the eigenvalue ω, the elements of which are derived in Appendix A.

Through repeated application of Eq. (19), the six constants in the first segment (A_1, B_1, C_1, D_1, E_1, and F_1) can be mapped into those of the last segment (A_K, B_K, C_K, D_K, E_K and F_K), thereby reducing the number of independent constants in the entire system to six:

$$\begin{Bmatrix} A_K \\ B_K \\ C_K \\ D_K \\ E_K \\ F_K \end{Bmatrix} = \mathbf{T}^{(K-1)}_{6\times 6} \begin{Bmatrix} A_{K-1} \\ B_{K-1} \\ C_{K-1} \\ D_{K-1} \\ E_{K-1} \\ F_{K-1} \end{Bmatrix} = \mathbf{T}^{(K-1)}_{6\times 6} \ldots \mathbf{T}^{(2)}_{6\times 6}\mathbf{T}^{(1)}_{6\times 6} \begin{Bmatrix} A_1 \\ B_1 \\ C_1 \\ D_1 \\ E_1 \\ F_1 \end{Bmatrix}. \tag{20}$$

Because of the characteristics of the closed structures, the relationship of the constants in the Kth segment (A_K, B_K, C_K, D_K, E_K and F_K) and the first segment (A_1, B_1, C_1, D_1, E_1, and F_1) can be expressed as (refer to Fig. 1)

$$\begin{Bmatrix} A_1 \\ B_1 \\ C_1 \\ D_1 \\ E_1 \\ F_1 \end{Bmatrix} = \mathbf{T}^{(K)}_{6\times 6} \begin{Bmatrix} A_K \\ B_K \\ C_K \\ D_K \\ E_K \\ F_K \end{Bmatrix}.$$

By substituting Eq. (20) into the above equation,

$$\begin{Bmatrix} A_1 \\ B_1 \\ C_1 \\ D_1 \\ E_1 \\ F_1 \end{Bmatrix} = \mathbf{T}^{(K)}_{6\times 6}\mathbf{T}^{(K-1)}_{6\times 6} \ldots \mathbf{T}^{(2)}_{6\times 6}\mathbf{T}^{(1)}_{6\times 6} \begin{Bmatrix} A_1 \\ B_1 \\ C_1 \\ D_1 \\ E_1 \\ F_1 \end{Bmatrix} = \mathbf{R}_{6\times 6} \begin{Bmatrix} A_1 \\ B_1 \\ C_1 \\ D_1 \\ E_1 \\ F_1 \end{Bmatrix}$$

$$= \begin{bmatrix} r_{11}(\omega) & r_{12}(\omega) & r_{13}(\omega) & r_{14}(\omega) & r_{15}(\omega) & r_{16}(\omega) \\ r_{21}(\omega) & \ldots & & & & r_{26}(\omega) \\ \vdots & & & & & \\ \vdots & & & & & \\ r_{61}(\omega) & & & & & r_{66}(\omega) \end{bmatrix} \begin{Bmatrix} A_1 \\ B_1 \\ C_1 \\ D_1 \\ E_1 \\ F_1 \end{Bmatrix},$$

where $\mathbf{R}_{6\times6} \equiv \mathbf{T}^{(K)}_{6\times6}\ \mathbf{T}^{(K-1)}_{6\times6} \ldots \mathbf{T}^{(2)}_{6\times6}\mathbf{T}^{(1)}_{6\times6}$ The above equation can then be expressed as

$$\mathbf{R}_{6\times6}\begin{Bmatrix} A_1 \\ B_1 \\ C_1 \\ D_1 \\ E_1 \\ F_1 \end{Bmatrix} - \begin{Bmatrix} A_1 \\ B_1 \\ C_1 \\ D_1 \\ E_1 \\ F_1 \end{Bmatrix} = (\mathbf{R}_{6\times6} - \mathbf{I}_{6\times6})\begin{Bmatrix} A_1 \\ B_1 \\ C_1 \\ D_1 \\ E_1 \\ F_1 \end{Bmatrix} = \mathbf{0}, \tag{21}$$

where $\mathbf{I}_{6\times6}$ is an identity matrix. Thus, the existence of non-trivial solutions requires

$$\det|\mathbf{R}_{6\times6} - \mathbf{I}_{6\times6}| = 0. \tag{22}$$

This determinant provides the single (characteristic) equation for the solution of the eigenvalue ω_n. When eigenvalues are obtained, the coefficients of the eigenfunctions, $w_{(n)}(x)$ and $v_{(n)}(x)$, are then determined by back-substitution into Eqs. (21) and (19) first and then into Eqs. (13) and (14).

4. Numerical results and discussion

The method for obtaining the eigenvalues (natural frequencies) proposed in this article is that of finding the non-trivial solutions of the determinant in Eq. (22). This is a nonlinear algebraic equation which can be solved by using the standard Newton–Raphson iterations or, for simplification, by using the method shown in Fig. 4 to obtain the eigenvalues.

The Timoshenko shear coefficient k in the governing equations (Eqs. (1) and (2)) is used to simplify the non-uniform shear stress distribution at a cross-section to retain the one-dimensional approach. There are virtually as many different definitions of k as there are published papers on the Timoshenko beam. Here, Cowper's definition of k, which is a function of a cross-section,

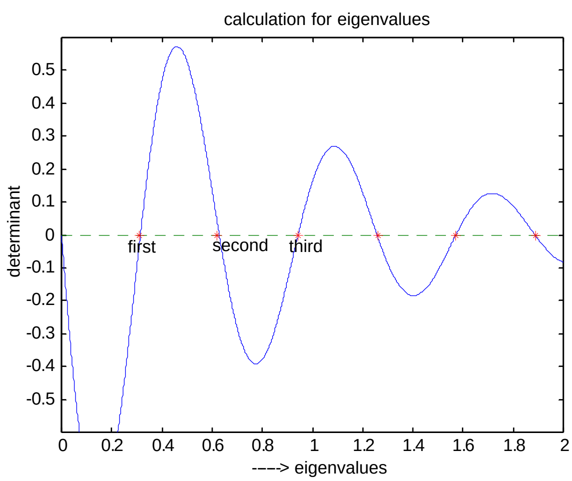

Fig. 4. Simple calculation of eigenvalues.

Poisson's ratio v [6], and for the case of the square cross-section used in this article, $k = 10(1+v)/(12+11v)$ are used. The Timoshenko beam model, in which the shear deformation effect has been considered, and, thus, its applications are much wider than those of the traditional Euler–Bernoulli beam model. When a beam is short enough, then the shear deformation effects cannot be ignored, in which case the results of the Euler–Bernoulli beam model are no longer valid.

In order to validate the method presented in this article, some numerical results are compared with the experimental data. First is the case of a triangular closed-frame structure, as shown in Fig. 5. The non-dimensional lengths and the frame angles are $l_1 = 0.293$, $l_2 = 0.293$, $l_3 = 0.414$, $\theta_1 = \pi/2$, $\theta_2 = \pi/4$, $\theta_3 = \pi/4$, the total length $L(= L_1 + L_2 + L_3)$ is 0.92 m. The square sectional dimensions and material properties are: section width, $B = 12.7$ mm; section height, $H = 12.7$ mm; density, $\rho = 7800\,\mathrm{kg/m^3}$; Young's modulus, $E = 2.06 \times 10^{11}\,\mathrm{N/m^2}$; shear modulus of elasticity, $G = 79 \times 10^9\,\mathrm{N/m^2}$; and Poisson's ratio, $v = 0.3$. This triangular frame structure is suspended by a rubber band, for which the setup of the test is shown in Fig. 6. An impact test is used by an impact hammer (load cell, PCB 208C02), an accelerometer (PCB 352 C65) and a dynamic signal analyzer (Stanford Research Systems, model SR785). The accelerator is located at the midpoint of the side and the impact hammer hits the other side (refer to Fig. 6). From the

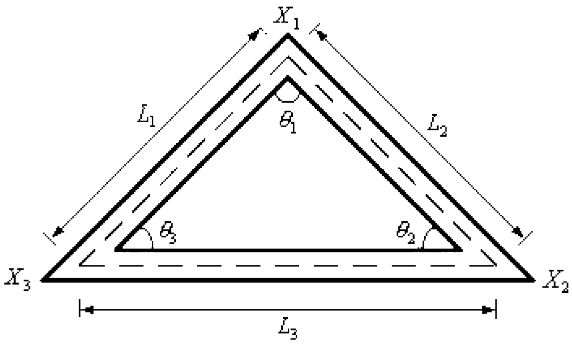

Fig. 5. A triangular frame structure, specifications of which appear in caption for Table 1.

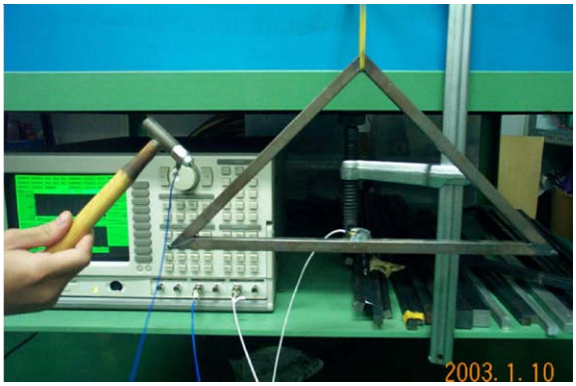

Fig. 6. Experimental modal testing of triangular frame structure.

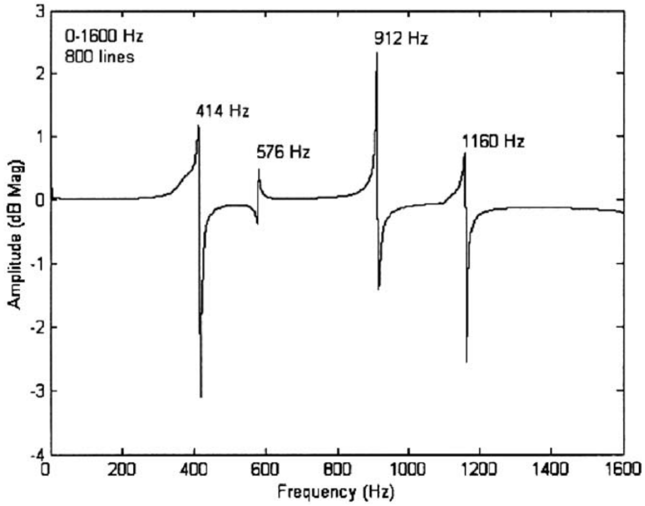

Fig. 7. Measured transfer function of triangular frame structure.

Table 1
Experimental comparisons

Measured natural frequencies (Hz)	Calculated natural frequencies (Hz)	Error (%)
$\Omega_1 =$ 414	414.28	0.07
$\Omega_2 =$ 576	587.69	2.03
$\Omega_3 =$ 912	907.41	0.50
$\Omega_4 =$ 1160	1162.91	0.25

Experimental comparisons of a triangular closed-frame structure with $l_1 = 0.293$, $l_2 = 0.293$, $l_3 = 0.414$, $\theta_1 = \pi/2$, $\theta_2 = \pi/4$, $\theta_3 = \pi/4$, a total length of $L(= L_1 + L_2 + L_3) = 0.92\,\mathrm{m}$, a section height of $H = 1.27\,\mathrm{cm}$, a section width of $B = 1.27\,\mathrm{cm}$, a density of $\rho = 7800\,\mathrm{kg/m^3}$, a Young's modulus of $E = 2.06 \times 10^{11}\,\mathrm{N/m^2}$, a shear modulus of elasticity of $G = 79 \times 10^9\,\mathrm{N/m^2}$and a Poisson's ratio of $\nu = 0.3$, shown in Fig. 5.

experimental modal testing, a transfer function is measured as shown in Fig. 7, from which the lowest four natural frequencies are obtained as $\Omega_1 = 414$, $\Omega_2 = 576$, $\Omega_3 = 912$, $\Omega_4 = 1160\,\mathrm{Hz}$. The comparisons of the calculated natural frequencies from this study and the measured results are shown in Table 1. From Table 1, it can be observed that the errors are small and satisfactory.

For another case of a square closed-frame structure with $l_1 = l_2 = l_3 = l_4 = 0.25, \theta_1 = \theta_2 = \theta_3 = \theta_4 = \pi/2$, a total length of $L(= L_1 + L_2 + L_3 + L_4) = 0.96\,\mathrm{m}$, the sectional dimensions and material properties are the same as in the aforementioned case. Table 2 shows the comparisons of numerical and experimental results. From Table 2, again, it can be observed that the errors are also small and acceptable.

When the eigenvalue (natural frequency) is obtained, the coefficients of the corresponding eigenfunction (mode shape), $w_{(n)}(x)$ and $v_{(n)}(x)$, can be determined by back-substitution into Eqs. (21) and (19) first and then into Eqs. (13) and (14). For the triangular closed-frame structure

Table 2
Experimental comparisons

Measured natural frequencies (Hz)	Calculated natural frequencies (Hz)	Error (%)
$\Omega_1 =$ 304	297.03	2.30
$\Omega_2 =$ 516	513.38	0.50
$\Omega_3 =$ 1192	1153.42	3.34

Experimental comparisons of a square closed-frame structure with $l_1 = l_2 = l_3 = l_4 = 0.25$, $\theta_1 = \theta_2 = \theta_3 = \theta_4 = \pi/2$, a total length of $L(= L_1 + L_2 + L_3 + L_4) = 0.96\,\text{m}$, a section height of $H = 1.27\,\text{cm}$, a section width of $B = 1.27\,\text{cm}$, a density of $\rho = 7800\,\text{kg/m}^3$, a Young's modulus of $E = 2.06 \times 10^{11}\,\text{N/m}^2$, a shear modulus of elasticity of $G = 79 \times 10^9\,\text{N/m}^2$and a Poisson's ratio of $v = 0.3$.

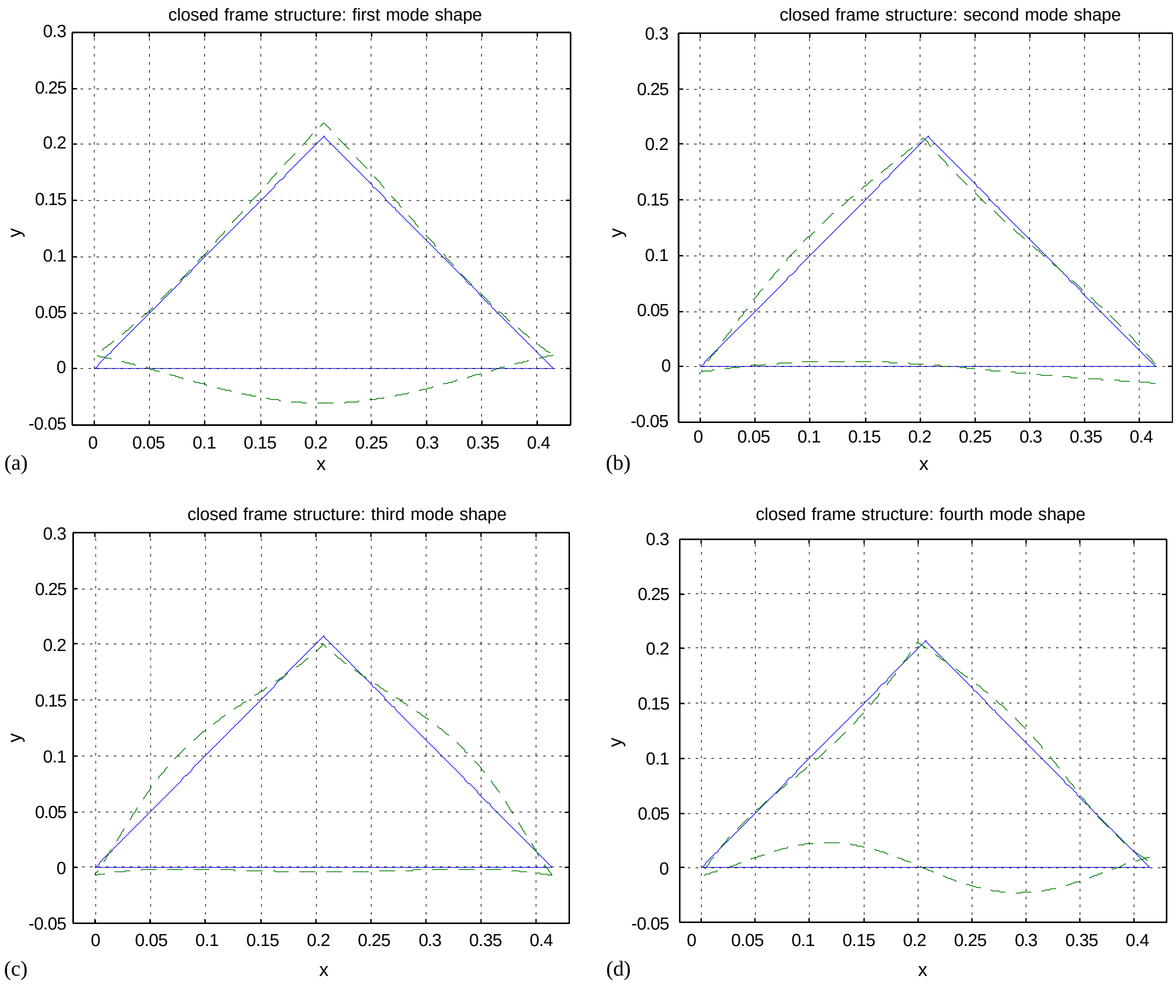

Fig. 8. Lowest four mode shapes of triangular frame structure.

shown in Fig. 5, by the solution procedure proposed in this article, the lowest four mode shapes are calculated as shown in Fig. 8a–d.

5. Conclusions

A hybrid analytical/numerical solution method has been developed that permits an efficient evaluation of eigensolutions for planar closed-frame structures. This method is based on modeling each sub-frame beam by the Timoshenko beam theory and considering the compatibility requirements across each frame angle. By using the analytical transfer matrix method, the characteristic equation of this system can be obtained. Eigensolutions can then be determined numerically by solving this characteristic equation. The method presented in this article is also validated by the data from the experimental modal testing. Unlike all the other methods, in which the dimensions of the matrix increase with the complexity of the structure, there are only six undetermined coefficients in the method proposed herein. The main feature of this method is that of decreasing the dimensions of the matrix involved in the finite element method and certain other analytical methods.

Acknowledgment

The author gratefully acknowledges the support of National Science Council in Taiwan ROC under Grant Number NSC 92-2212-E-212-021. The author also wishes to express appreciation to Dr. Cheryl Rutledge for her editorial assistance.

Appendix A. Transfer matrix derivation

The compatibility conditions across the ith angle ($i = 1, 2, ..., K$) are represented in Eqs. (18a)–(18f).

From Eq: (18a):

$$
\begin{aligned}
w_{(i+1)}(x_i^+) &= -w_{(i)}(x_i^-)\cos\theta_i + v_{(i)}(x_i^-)\sin\theta_i \\
\rightarrow A_{i+1} + C_{i+1} = &- (A_i \cosh\lambda_1 l_i + B_i \sinh\lambda_1 l_i + C_i \cos\lambda_2 l_i + D_i + \sin\lambda_2 l_i)\cos\theta_i \\
&+ (E_i \sin\gamma l_i + F_i \cos\gamma l_i)\sin\theta_i, \qquad i = 1, 2, ..., K.
\end{aligned}
\tag{A.1}
$$

From Eq. (18b):

$$
\begin{aligned}
v_{(i+1)}(x_i^+) &= -w_{(i)}(x_i^-)\sin\theta_i - v_{(i)}(x_i^-)\cos\theta_i, \\
\rightarrow F_{i+1} = &- (A_i \cosh\lambda_1 l_i + B_i \sinh\lambda_1 l_i + C_i \cos\lambda_2 l_i + D_i \sin\lambda_2 l_i)\sin\theta_i \\
&- (E_i \sin\gamma l_i + F_i \cos\gamma l_i)\cos\theta_i, \qquad i = 1, 2, ..., K.
\end{aligned}
\tag{A.2}
$$

From Eq. (18c):

$$
\begin{aligned}
& w'_{(i+1)}(x_i^+) = w'_{(i)}(x_i^-), \\
\to\ & B_{i+1}\lambda_1 + D_{i+1}\lambda_2 = A_i\lambda_1 \sinh\lambda_1 l_i + B_i\lambda_1 \cosh\lambda_1 l_i \\
& \qquad - C_i\lambda_2 \sin\lambda_2 l_i + D_i\lambda_2 \cos\lambda_2 l_i, \quad i = 1, 2, \ldots, K.
\end{aligned}
\tag{A.3}
$$

From Eq. (18d):

$$
\begin{aligned}
& \varphi'_{(i+1)}(x_i^+) = \varphi'_{(i)}(x_i^-), \\
\to\ & A_{i+1}q_1\lambda_1 + C_{i+1}q_2\lambda_2 = A_i q_1\lambda_1 \cosh\lambda_1 l_i + B_i q_1\lambda_1 \sinh\lambda_1 l_i \\
& \qquad + C_i q_2\lambda_2 + \cos\lambda_2 l_i + D_i q_2\lambda_2 \sin\lambda_2 l_i, \quad i = 1, 2, \ldots, K.
\end{aligned}
\tag{A.4}
$$

From Eq. (18e):

$$
\begin{aligned}
& w'_{(i+1)}(x_i^+) - \varphi_{(i+1)}(x_i^+) = -[w'_{(i)}(x_i^-) - \varphi_{(i)}(x_i^-)]\cos\theta_i + \frac{E}{kG}v'_{(i)}(x_i^-)\sin\theta_i, \\
& \to B_{i+1}\lambda_1 + D_{i+1}\lambda_2 - (B_{i+1}q_1 - D_{i+1}q_2) \\
& \quad = -[(A_i\lambda_1 \sinh\lambda_1 l_i + B_i\lambda_1 \cosh\lambda_1 l_i - C_i\lambda_2 \sin\lambda_2 l_i + D_i\lambda_2 \cos\lambda_2 l_i) \\
& \qquad - (A_i q_1 \sinh\lambda_1 l_i + B_i q_1 \cosh\lambda_1 l_i + C_i q_2 \sin\lambda_2 l_i - D_i q_2 \cos\lambda_2 l_i)]\cos\theta_i \\
& \qquad + \frac{E}{kG}(E_i\gamma\cos\gamma l_i - F_i\gamma\sin\gamma l_i)\sin\theta_i, \qquad i = 1, 2, \ldots, K.
\end{aligned}
\tag{A.5}
$$

From Eq. (18f):

$$
\begin{aligned}
v'_{(i+1)}(x_i^+) = & -\frac{kG}{E}[w'_{(i)}(x_i^-) - \varphi_{(i)}(x_i^-)]\sin\theta_i - v'_{(i)}(x_i^-)\cos\theta_i, \\
\to E_{i+1}\gamma = & -\frac{kG}{E}[(A_i\lambda_1\sinh\lambda_1 l_i + B_i\lambda_1\cosh\lambda_1 l_i - C_i\lambda_2\sin\lambda_2 l_i + D_i\lambda_2\cos\lambda_2 l_i) \\
& - (A_i q_1\sinh\lambda_1 l_i + B_i q_1\cosh\lambda_1 l_i + C_i q_2\sin\lambda_2 l_i - D_i q_2\cos\lambda_2 l_i)]\sin\theta_i \\
& - (E_i\gamma\cos\gamma l_i - F_i\gamma\sin\gamma l_i)\cos\theta_i, \qquad i = 1, 2, \ldots, K.
\end{aligned}
\tag{A.6}
$$

Solving for Eqs. (A.1)–(A.6) leads to the following recursion formulae for the constants $A_{i+1}, B_{i+1}, C_{i+1}, D_{i+1}, E_{i+1}$ and F_{i+1} :

$$
\begin{Bmatrix} A_{i+1} \\ B_{i+1} \\ C_{i+1} \\ D_{i+1} \\ E_{i+1} \\ F_{i+1} \end{Bmatrix} = \begin{bmatrix} t_{11} & t_{12} & t_{13} & t_{14} & t_{15} & t_{16} \\ \vdots & & & & & \\ \vdots & & & & & \\ \ldots\ldots\ldots\ldots & & & & ..t_{65} & t_{66} \end{bmatrix}^{(i)} \begin{Bmatrix} A_i \\ B_i \\ C_i \\ D_i \\ E_i \\ F_i \end{Bmatrix} = \mathbf{T}_{6\times 6}^{(i)} \begin{Bmatrix} A_i \\ B_i \\ C_i \\ D_i \\ E_i \\ F_i \end{Bmatrix}, \quad i = 1, 2, \ldots, K.
$$

Here, $\mathbf{T}^{(i)}_{6\times 6}$ is a transfer matrix composed of the elements:

$$t_{11} = \frac{q_2\lambda_2}{q_1\lambda_1 - q_2\lambda_2}\left(\frac{q_1\lambda_1}{q_2\lambda_2} + \cos\theta_i\right)\cosh\lambda_1 l_i, \qquad t_{12} = -\frac{q_2\lambda_2}{q_1\lambda_1 - q_2\lambda_2}\left(\frac{q_1\lambda_1}{q_2\lambda_2} + \cos\theta_i\right)\sinh\lambda_1 l_i,$$

$$t_{13} = \frac{q_2\lambda_2}{q_1\lambda_1 - q_2\lambda_2}(1+\cos\theta_i)\cos\lambda_2 l_i, \qquad t_{14} = \frac{q_2\lambda_2}{q_1\lambda_1 - q_2\lambda_2}(1+\cos\theta_i)\sin\lambda_1 l_i,$$

$$t_{15} = -\frac{q_2\lambda_2}{q_1\lambda_1 - q_2\lambda_2}\sin\gamma l_i\sin\theta_i, \qquad t_{16} = -\frac{q_2\lambda_2}{q_1\lambda_1 - q_2\lambda_2}\cos\gamma l_i\sin\theta_i,$$

$$t_{21} = \frac{\lambda_2}{q_1\lambda_2 + q_2\lambda_1}\left(\frac{\lambda_1}{\lambda_2}q_2 + \lambda_1 + \lambda_1\cos\theta_i - q_1\cos\theta_i\right)\sinh\lambda_1 l_i,$$

$$t_{22} = \frac{\lambda_2}{q_1\lambda_2 + q_2\lambda_1}\left(\frac{\lambda_1}{\lambda_2}q_2 + \lambda_1 + \lambda_1\cos\theta_i - q_1\cos\theta_i\right)\cos\lambda_1 l_i,$$

$$t_{23} = -\frac{\lambda_2}{q_1\lambda_2 + q_2\lambda_1}(1+\cos\theta_i)(q_2+\lambda_2)\sin\lambda_2 l_i, \qquad t_{24} = \frac{\lambda_2}{q_1\lambda_2 + q_2\lambda_1}(1+\cos\theta_i)(q_2+\lambda_2)\cos\lambda_2 l_i,$$

$$t_{25} = -\frac{\lambda_2}{q_1\lambda_2 + q_2\lambda_1}\frac{E}{kG}\gamma\cos\gamma l_i\sin\theta_i, \qquad t_{26} = \frac{\lambda_2}{q_1\lambda_2 + q_2\lambda_1}\frac{E}{kG}\gamma\sin\gamma l_i\sin\theta_i,$$

$$t_{31} = \frac{q_1\lambda_1}{q_2\lambda_2 - q_1\lambda_1}(1+\cos\theta_i)\cosh\lambda_1 l_i, \qquad t_{32} = \frac{q_1\lambda_1}{q_2\lambda_2 - q_1\lambda_1}(1+\cos\theta_i)\sin\lambda_1 l_i,$$

$$t_{33} = \frac{q_1\lambda_1}{q_2\lambda_2 - q_1\lambda_1}\left(\frac{q_2\lambda_2}{q_1\lambda_1} + \cos\theta_i\right)\cos\lambda_2 l_i, \qquad t_{34} = \frac{q_1\lambda_1}{q_2\lambda_2 - q_1\lambda_1}\left(\frac{q_2\lambda_2}{q_1\lambda_1} + \cos\theta_i\right)\sin\lambda_2 l_i,$$

$$t_{35} = \frac{q_1\lambda_1}{q_2\lambda_2 - q_1\lambda_1}\sin\gamma l_i\sin\theta_i, \qquad t_{36} = -\frac{q_1\lambda_1}{q_2\lambda_2 - q_1\lambda_1}\cos\gamma l_i\sin\theta_i,$$

$$t_{41} = \frac{\lambda_1}{q_1\lambda_2 + q_2\lambda_1}(1+\cos\theta_i)(q_1-\lambda_1)\sinh\lambda_1 l_i, \qquad t_{42} = \frac{\lambda_1}{q_1\lambda_2 + q_2\lambda_1}(1+\cos\theta_i)(q_1-\lambda_1)\cosh\lambda_1 l_i,$$

$$t_{43} = -\frac{\lambda_1}{q_1\lambda_2 + q_2\lambda_1}\left(\frac{\lambda_2}{\lambda_1}q_1 - \lambda_2 - \lambda_2\cos\theta_i - q_2\cos\theta_i\right)\sin\lambda_2 l_i,$$

$$t_{44} = \frac{\lambda_1}{q_1\lambda_2 + q_2\lambda_1}\left(\frac{\lambda_2}{\lambda_1}q_1 - \lambda_2 - \lambda_2\cos\theta_i - q_2\cos\theta_i\right)\cos\lambda_2 l_i,$$

$$t_{45} = \frac{\lambda_1}{q_1\lambda_2 + q_2\lambda_1}\frac{E}{kG}\gamma\cos\gamma l_i\sin\theta_i, \qquad t_{46} = -\frac{\lambda_1}{q_1\lambda_2 + q_2\lambda_1}\frac{E}{kG}\gamma\sin\gamma l_i\sin\theta_i,$$

$$t_{51} = \tfrac{kG}{E\gamma}(q_1-\lambda_1)\sinh\lambda_1 l_i\sin\theta_i, \qquad t_{52} = \tfrac{kG}{E\gamma}(q_1-\lambda_1)\cosh\lambda_1 l_i\sin\theta_i,$$

$$t_{53} = \tfrac{kG}{E\gamma}(\lambda_2+q_2)\sin\lambda_2 l_i\sin\theta_i, \qquad t_{54} = \tfrac{kG}{E\gamma}(\lambda_2+q_2)\cos\lambda_2 l_i\sin\theta_i,$$

$$t_{55} = -\cos\gamma l_i\cos\theta_i, \qquad t_{56} = \sin\gamma l_i\cos\theta_i,$$

$$t_{61} = -\cosh \lambda_1 l_i \sin \theta_i, \qquad t_{62} = -\sinh \lambda_1 l_i \sin \theta_i,$$
$$t_{63} = -\cos \lambda_2 l_i \sin \theta_i, \qquad t_{64} = -\sin \lambda_2 l_i \sin \theta_i,$$
$$t_{65} = -\sin \gamma l_i \cos \theta_i, \qquad t_{66} = -\cos \gamma l_i \cos \theta_i.$$

References

[1] A.Y.T. Leung, Dynamic stiffness for structures with distributed deterministic or random loads, *Journal of Sound and Vibration* 242 (3) (2001) 377–395.
[2] D.H. Moon, M.S. Choi, Vibration analysis for frame structures using transfer of dynamic stiffness coefficient, *Journal of Sound and Vibration* 234 (5) (2000) 725–736.
[3] N.S. Sehmi, *Large Order Structural Eigenanalysis Techniques Algorithm for Finite Element Systems*, Ellis Horwood, New York, 1989.
[4] M. Geradin, S.L. Chen, An exact model reduction technique for beam structures: combination of transfer and dynamic stiffness matrices, *Journal of Sound and Vibration* 185 (3) (1995) 431–440.
[5] M. Ohga, T. Shigematsu, T. Hara, Structural analysis by a combined finite element transfer matrix method, *Computers and Structures* 17 (1983) 321–326.
[6] I.J. Shames, C.L. Dym, *Energy and Finite Element Methods in Structural Mechanics*, McGraw-Hill, New York, 1985.
[7] L. Meirovitch, *Fundamentals of Vibrations*, McGraw-Hill Higher Education, Singapore, 2001.
[8] W.C. Hurty, M.F. Rubinstein, *Dynamics of Structures*, Prentice-Hall, Englewood Cliffs, NJ, 1964.
[9] L. Meirovitch, *Elements of Vibration Analysis*, McGraw-Hill, Singapore, 1986.
[10] T.C. Tsai, Y.Z. Wang, Vibration analysis and diagnosis of a cracked shaft, *Journal of Sound and Vibration* 192 (3) (1996) 607–620.
[11] H.P. Lin, N.C. Perkins, Free vibration of complex cable/mass system: theory and experiment, *Journal of Sound and Vibration* 179 (1) (1995) 131–149.
[12] H.P. Lin, C.K. Chen, Analysis of cracked beams by transfer matrix method. *The 25th National Conference on Theoretical and Applied Mechanics*, Taichung, Taiwan, 2001, pp. 3123–3132.
[13] H.P. Lin, J. Ro, Vibration analysis of planar serial-frame structures, *Journal of Sound and Vibration* 262 (5) (2003) 1113–1131.